Self-generated magnetic field and Faraday rotation in a laser-produced plasma

Manoranjan Khan, C. Das, and B. Chakraborty
Centre for Plasma Studies, Faculty of Science, Jadavpur University, Calcutta 700032, India

T. Desai and H. C. Pant
Laser Programme, Centre for Advanced Technology, Indore 452013, India

M. K. Srivastava and S. V. Lawande
Theoretical Physics Division, Bhabha Atomic Research Centre, Mumbai 400085, India
(Received 1 October 1997)

In laser-produced plasma the self-generated magnetic field can be excited by a collisional as well as a noncollisional process via ponderomotive action. In this paper we estimate the self-generated axial magnetic field by measuring the change in the polarization of stimulated Brillouin scattered (SBS) radiation as compared to the incident laser radiation. Experiments were conducted using a Nd:glass laser ($\lambda = 1.06\ \mu$m) capable of delivering a plane-polarized output of 20 J in 5 ns. The experimentally observed rotation of the plane of polarization of the SBS radiation has been shown to be in fairly good agreement with the estimated values from theory. [S1063-651X(98)04306-2]

PACS number(s): 52.50.Jm, 52.35.Mw

I. INTRODUCTION

A large number of mechanisms have been reported [1–12] for the generation of a large-scale magnetic field in laser-produced plasmas. The most important mechanisms are (i) magnetic field due to ponderomotive force [1], (ii) $\vec{\nabla} n \times \vec{\nabla} T$ mechanism [2–5], (iii) inverse Faraday effect (IFE) mechanism [5,8,9], and (iv) dynamo mechanism [11]. Although magnetic-field generation by different mechanisms is a simultaneous process, some mechanisms are dominant at a particular experimental condition and others are not. Here we report one of these mechanisms for the field generation in our experimental setup.

Ponderomotive force due to a spatially inhomogeneous laser beam is an effective mechanism for generating the magnetic field. In an interaction of an ultraintense short laser pulse with an overdense plasma target, the spatial gradient and nonstationary character of ponderomotive force can generate [13,14] a transverse magnetic field of the order of 10^9 G.

The ponderomotive force due to a spatially inhomogeneous laser beam constitutes an important mechanism of generating an axial magnetic field. It is shown by Srivastava *et al.* [1] that a magnetic field in the range of kilogauss may be generated by the ponderomotive action in a plasma produced by an obliquely incident laser [7] and the collisional contribution to the axial magnetic field generated by ponderomotive action is dominant over the noncollisional contribution when a lower intensity (I) and shorter wavelength (λ) laser is used. The axial field is typically of the order of a few kilogauss and scales as λ^{-2}. On the other hand, for a high intensity and longer wavelength laser, the noncollisional contribution arising from the spatial inhomogenities of the plasma is dominant and can be of the order of 0.5–0.6 MG. This field scales as $I^{4/3}\lambda^{14/3}$. Consistent with out experimental study, we are interested in a short wavelength and lower laser intensity region where collisions are prominent in the plasma.

Faraday rotation is the rotation of the plane of polarization of an electromagnetic wave when it passes through a magnetic field. In this paper, we will discuss an experiment to measure Faraday rotation of the incident laser radiation from laser-produced plasma and a plausible theoretical explanation. In fact, this work can be taken as experimental evidence for axial field generation at low laser intensity as predicted in an earlier theoretical paper [1].

It is also necessary to discuss certain results of the theory [1]. It has been shown that the polarization of an obliquely incident laser radiation undergoes rotation as it propagates to the turning point density layer and on its way back, i.e., specularly reflected radiation is once again rotated by an equal amount. Here, the instantaneous plasma conditions for a specularly reflected beam have been simplified by not considering the various local effects and their role on the specularly reflected beam at the turning point plasma density layer.

Various authors have analyzed the critical density plasma conditions [15–17] for $\theta = 0$. In our recent specular studies, we have shown the effect of the turning point plasma layer on specular reflection [17].

Stamper *et al.* [2] used a probe beam transverse to the expanding plasma and the characteristics of the transmitted beam to measure the self-generated magnetic field. In the case of an axial measurement, we must use the probe beam along the laser axis. Therefore, the stimulated Brillouin scattering (SBS) study provides a simple and reliable technique for measuring the self-generated axial magnetic field. The axial magnetic field can be effective on SBS since most of the SBS grows until it reaches the turning point density and reflects back exactly along the path of incidence. The estimated values remain unaffected for SBS studies. In this paper we experimentally estimate the self-generated axial magnetic field by measuring the polarization of SBS and comparing it with the incident laser radiation.

II. THEORY

Irradiation of a plane, optically polished copper target with a 5 ns laser beam ($I \approx 10^{13}$ W/cm^2) produces an expanding plasma over the laser pulse duration. This plasma interacts with the inward propagating laser beam. Laser radiation is absorbed by a classical mechanism up to the critical density layer and simultaneously undergoes reflection prominantly by SBS, specular reflection, and stimulated Raman scattering (SRS).

The intensity threshold for SBS [18] is $I \approx 10^{12}$ W/cm^2 under our experimental condition. SRS is neglected since the threshold intensity for SRS is $>10^{14}$ W/cm^2 (Ref. [7]). Laser plasma interaction gives rise to a large axial magnetic field. The generation of the magnetic field can be explained as follows.

We consider a plasma consisting of a single ion species of charge Z, mass M, and electrons of mass m. The basic equations describing the motion of the plasma, interacting with an incident electromagnetic wave, are

$$\partial_t(n_j) + \vec{\nabla}\cdot(n_j\vec{V}_j) = 0, \tag{1}$$

$$mn_e D_e(\vec{V}_e) = -\vec{\nabla}(n_e T_e) - n_e e(\vec{E} + \vec{V}_e \times \vec{B}) - mn_e \nu(\vec{V}_e - \vec{V}_i), \tag{2}$$

$$Mn_i D_i(\vec{V}_i) = -\vec{\nabla}(n_i T_i) + Zn_i e(\vec{E} + \vec{V}_i \times \vec{B}) + mn_e \nu(\vec{V}_e - \vec{V}_i), \tag{3}$$

where n_j, $\vec{V}_j$, and T_j $(j = e,i)$ are densities, velocities, and temperatures of the electrons and ions, respectively, and $D_j = \partial_t + (\vec{V}_j \cdot \nabla)$ is the usual convective derivative. Here we assume that momentum exchange takes place only between the electrons and ions via elastic collisions with frequency ν and no momentum is lost by any other dissipative process. Here $\vec{E}$ and $\vec{B}$ are the self-consistent electric and magnetic fields in the plasma given by the following Maxwell equations:

$$\vec{\nabla}\times\vec{E} = -\partial_t(\vec{B}), \tag{4}$$

$$\vec{\nabla}\times\vec{B} = -c^{-2}\partial_t(\vec{E}) + \mu_0\vec{J}, \tag{5}$$

$$\vec{\nabla}\cdot\vec{E} = \rho/\epsilon_0, \tag{6}$$

$$\vec{\nabla}\cdot\vec{B} = 0, \tag{7}$$

$$\rho = e(n_i Z - n_e), \tag{8}$$

$$\vec{J} = e(n_i Z\vec{V}_i - n_e\vec{V}_e), \tag{9}$$

where e the electron charge, c is the speed of light in vacuum, while ϵ_0 and μ_0 are the dielectric permitivity and permeability in free space, respectively. Here ∂_t in the above equations represents the partial derivative with respect to time t.

Based on these equations, the existence of ponderomotive force and hence the axial magnetic field has been calculated and reported by us [1] in 1992. The growth rates of various components of the magnetic fields are given in Eqs. (36)–(38) in the published paper [1].

The axial field B_{OX} has two parts, one collisional B^c_{OX} and the other noncollisional $B^{\rm nc}_{OX}$,

$$B_{OX} = B^c_{OX} + B^{\rm nc}_{OX}. \tag{10}$$

These are given as

$$B^c_{OX} = -\frac{et_0}{2mw^2}\left(\frac{\nu}{e}\sin\theta_0 f_a \frac{\partial A^2}{\partial Z}\right). \tag{11}$$

As mentioned in Ref. [1], for an inhomogeneous plasma, the flow variables are slowly varying functions of space and the electric field may be expressed as

$$\vec{E} = \vec{A}(r)\exp\{i\psi(r)\},$$

where ψ is complex and called eikonal, amplitude A is real, and

$$\{A, \partial x(A)\} = \frac{\partial A}{\partial Z}\frac{\partial^2 A}{\partial x\partial y} - \frac{\partial A}{\partial y}\frac{\partial^2 A}{\partial x\partial z}, \tag{12}$$

$$\{A, \partial y(A)\} = \frac{\partial A}{\partial Z}\frac{\partial^2 A}{\partial y^2} - \frac{\partial A}{\partial y}\frac{\partial^2 A}{\partial y\partial z}, \tag{13}$$

where t_0 is the pulse duration and m is the electron mass, w is the laser frequency, ν is the collisional frequency between electron and ions, θ_0 is the angle of the incidence outside the plasma, and f_t is the transmission factor of the incident laser radiation in the plasma due to collision between electrons and ions, such that $f_t = 1 - f_a$, where f_a is the fraction of radiation absorption given as

$$f_a = \exp\left(-\int K(x)dx\right), \tag{14}$$

where

$$K(x) = \frac{\nu N_0(x)}{e\mu(x)}, \quad \mu(x) = [1 - N_0(x)]^{1/2} : N_0(x) = \frac{n_0(X)}{n_c}. \tag{15}$$

A is the amplitude of the electric field and it is a vector quantity, $g = d\lambda_D^2/dx$, where λ_D is the Debye length and dimensionless factor $H(X) = (\cos^2\theta_0 - N_0)^{1/2}$, and N_0 is the ratio of the charge density to the critical surface density.

It is seen from Eq. (11) that for normal incidence ($\theta = 0$), the ponderomotive force does not excite an axial magnetic field. However, it can still excite a transverse magnetic field, which is not of interest for the present work. Moreover, collisional excitation is the only mechanism that gives rise to the axial field in the absence of density inhomogeneity (i.e., $g = 0$). However, in a laser-produced plasma, even at normal incidence, the axial field can appear [8,9,19] due to density inhomogeneity and collisions.

It has already been shown in Ref. [1] that for s-polarized light $B^{\rm nc}_{OX} = 0$ and it is the only collisional part that excites the axial magnetic field. In the absence of collisions, only higher-order noncollisional terms would contribute to the magnetic field, which is extremely small.

The presence of an axial magnetic field rotates the plane of polarization of the incident laser beam due to the Faraday

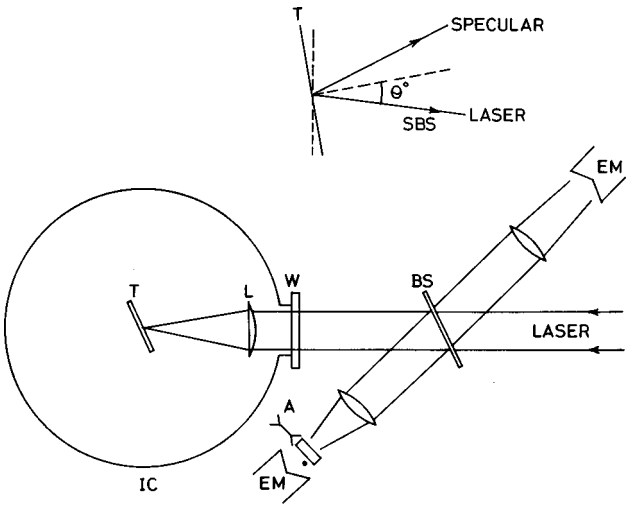

FIG. 1. Schematic of the experimental setup. IC, interaction chamber; *W*, glass window; BS, beam splitter; EM, energy meter; *A*, analyzer; inset, reflection of incident laser radiation due to stimulated Brillouin scattering and specular reflection.

effect. This rotation occurs in the subdense plasma in which the plasma density, temperature, and self-generated magnetic fields are varying in the axial direction. For the convenience of numerical calculations, the space has been divided into a finite number of slabs along the axial direction. In each slab the density and hence the magnetic field have been assumed to be fairly constant in space. The total Faraday rotation in the whole space is taken as the sum total of the Faraday rotation caused by each slab. The net rotation is then taken as $\alpha=\Sigma_{l=1}^{q}\,\alpha_l$, where $\alpha_l=B_l\Delta R_l$ is the rotation due to the lth slab, B_l being the corresponding axial magnetic field in the megagauss unit, ΔR_l is the slab thickness in micrometers, and q is a finite number.

III. EXPERIMENT

Experiments were performed using a 20 J, 5 ns Nd:glass laser (wavelength $\lambda=1.06\ \mu$m). The target was a massive plane polished copper slab, held on a specially designed target holder and placed at the center of an evacuated interaction chamber (Fig. 1). The target holder had a fine vertical movement so that a fresh target surface for every laser shot is available without disturbing the laser focusing conditions. The laser beam was irradiated at the target surface using an aspheric lens with a focal length of 50 cm. A small fraction (8%) of the incident beam was reflected from a beam splitter before entering the focusing lens and the interaction chamber. This fraction of the laser energy was used for estimating the incident laser energy on the target surface. The same beam splitter was also used for collecting SBS laser light from the target. The laser focal spot at the target surface was 160 μm [full width at half maximum (FWHM)] and 80% of the laser energy was contained within it.

The incident laser beam was *s*-polarized. Nevertheless, care was taken to avoid depolarization effects from glass laser amplifiers. For this purpose a multilayer thin-film polarizer was placed at the exit of the laser chain, assuring the plane of polarization of the incident laser beam. The target plane was rotated by 22.5° to the laser axis ($\theta=22.5$) so that

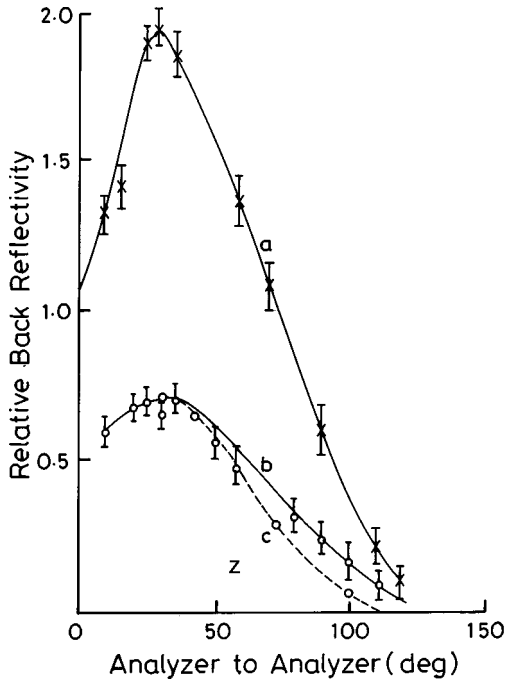

FIG. 2. Variation of relative backreflectivity as a function of the angle of the analyzer for (a) glass and (b) Copper target. Theoretical values are represented by dotted lines (c) for the copper target.

only stimulated Brillouin backscattered laser radiation, as in Fig. 1 (inset), was collected by the focusing lens. Thus the contribution due to the specularly reflected radiation to the SBS measurement was avoided.

The polarization of the incident laser was ascertained using a rotatable sheet analyzer (*A* in Fig. 1) placed at the front of the SBS detector (laser calorimeter). To study the effect of the copper plasma on the polarization of the laser beam, we measured SBS polarization. For comparative study, initially a flat glass surface was placed in front of the focusing lens (no target inside the chamber). It is known that the glass surface reflects the incident beam without changing the initial polarization. The glass surface was irradiated with low laser intensity to avoid plasma formation. The backreflected radiation showed no change in the polarization as compared to the incident radiation. This confirmed that there is no polarization change induced by any component of the experimental setup. By rotating the analyzer, the polarization characteristics of the SBS radiation were obtained keeping the constant angle of incidence as in Fig. 2(a). The polarization characteristics of the SBS from the copper target plasma at an incident laser intensity of $\sim 5\times10^{12}$ W/cm^2 were recorded [Fig. 2(b)].

IV. NUMERICAL SIMULATIONS

In order to estimate the magnetic field, the density and temperature profiles are numerically calculated using a 2D hydrodynamic code, castor-2. The incident laser profile has been assumed to have a rise time of 1 ns, which is consistent with our experimental conditions and for simplicity it was taken as Gaussian. The pulse duration was 5 ns (FWHM) and peak laser intensity is $I=5\times10^{12}$ W/cm^2. At this intensity, in case of the copper target, the total *X*-radiation emission is

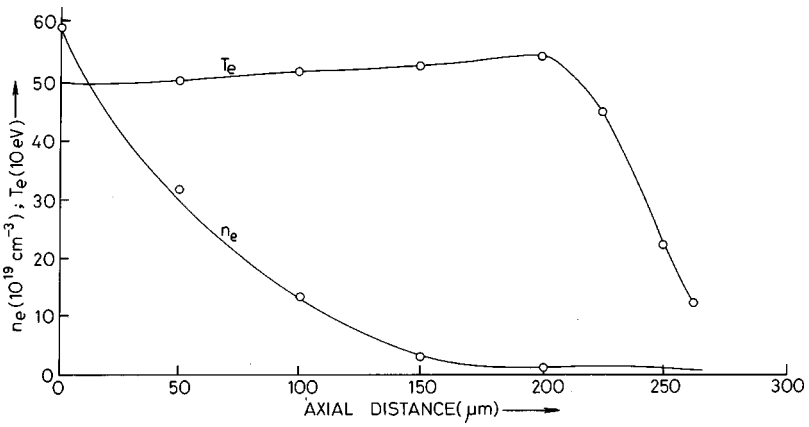

FIG. 3. Profiles of electron density (n_e) and temperature (T_e) of laser-produced plasma along the axial direction according to 2D hydrodynamic code simulations.

10% and hence its effect on density and temperature profile is neglected.

To compute the Faraday rotation angle ($\alpha = \Sigma_{l=1}^{q} B_l \Delta R_l$), we have restricted our calculation to a distance of 210 μm from the critical density surface due to the following reasons.

The entire region under consideration has been assumed to be composed of slabs and the length ΔR of each slab is chosen such that the temperature in that slab is fairly constant and the mean value of the density can be reasonably taken. The induced magnetic field has been calculated on the basis of these values of temperature and density. Consequently, the product $B_l\,\Delta R_l$ has been calculated over each slab. B_l has been seen to be fairly constant over the slab length.

V. RESULTS AND DISCUSSIONS

Theoretically, the transmitted intensity should be proportional to $\cos^2$ (angle between plane of polarization and analyzer). This theoretical cosine distribution curve is drawn in Fig. 2. Figure 2(a) represents the experimental data of SBS from a laser-irradiated glass target surface, collected at different angles of the analyzer. These results coincide with the theoretically estimated cosine distribution of a reflected beam. Figure 2(b) shows similar data for a copper plasma and Fig. 2(c) is the theoretical cosine distribution. The experimental values marked with circles in the curve deviate from the ideal cosine curve.

It is clear from these curves [Fig. 2(b)] that the plane of polarization of the incident laser radiation undergoes depolarization, observed as deviation from the theoretical distribution curve near the minimum, and also a rotation at the peak as compared to the glass target.

There are two distinct features of the experimental curve. (i) Rotation of the plane of polarization of the incident beam due to SBS mechanism by 8°. (ii) The depolarization of the SBS by 8–10 % as seen from the crossed position of the analyzer (90°). Such depolarization can be explained by considering the randomly fluctuating self-generated magnetic fields at the turning point plasma density layer ($n_e = n_C \cos^2\theta$). In our earlier work [17] on the study of specular reflection, the depolarization ($\approx 10\%$) at $I = 5 \times 10^{12}$ W/cm^2 has been observed and explained. The depolarization of SBS at $\theta = 0$ of the analyzer may also occur, but these values are within the error bars of the experimental data.

The following theoretical interpretation explains the experimental results on the rotation of the plane of polarization of the incident laser beam due to SBS mechanism. Steady-state profiles of axial plasma density (n_e) and plasma temperature (T_e) are estimated using a 2D hydrodynamic code caster-2 simulation.

The density and temperature profiles are shown in Fig. 3. Temperature is seen steeply decaying over the region whereas the density is decaying rather slowly beyond the distance of 210 μm from the critical density surface. So it is difficult to choose a slab length in this region even of the order of 5 μm over which the mean value of temperature and density may be reasonably chosen. Moreover, the percentage of absorbed laser intensity becomes very small (1–2 %) below the density 10^{25}/m^3. Therefore, the calculated axial B_l field over a narrow slab length ΔR_l should be small and the product $B_l\,\Delta R_l$ will also be very small, thus the finite sum $\Sigma_{l=1}^{q}\,\Delta R_l$ in this region can be neglected.

However, in this region, where temperature and density gradients are high, a toroidal magnetic field (arising from $\vec{\nabla} n \times \vec{\nabla} T$) may be generated. But the Faraday rotation angle of the SBS beams is only due to axial field and thus cannot be affected by the toroidal field.

Here, we have calculated the self-generated axial magnetic field and computed the Faraday rotation angle $\alpha = \Sigma_{l=1}^{q} \Delta R_l$, considering the motion of electrons that contribute dominantly in laser-produced plasmas. From our experimental conditions we have $\lambda_L = 1.06$ μm, $\theta_0 = 22.5°$, $t_0 = 5 \times 10^{-9}$ s, $Z_{\text{eff}} = 15$ (for Cu), $T_{\text{KeV}} = 0.5$, $L_E = 10$ μm, and $L_n = 80$ μm, where λ_L is the wavelength of the laser beam, θ_0 is the incident angle, t_0 is the pulse duration, Z_{eff} is the effective ionization, T_{KeV} is the electron temperature in KeV, L_E is the scale length of the electric intensity vector variation, and L_n is the scale length of density variation that is equal to the spot radius.

Using these data in Eq. (11) we have

TABLE I. Numerical computation of Faraday rotation angle. X is the distance measured from critical density surface along axial direction. $X=-L_n \ln(N_0)$.

X in μm	dx in μm	N_O	f_t	$B_{OX}=538.1$ $N_0 f_t$	$\delta\alpha=-0.9126$ $N_0^2 f_t dx$
12.66		0.8536	0.075	34.44	0.258
	5.19				
17.85		0.80	0.15	64.57	0.452
	5.16				
23.01		0.70	0.205	77.22	0.506
	5.52				
28.53		0.60	0.275	88.78	0.535
	5.93				
34.46		0.50	0.4	107.62	0.584
	6.41				
40.87		0.40	0.6	129.14	0.608
	6.95				
47.82		0.30	0.74	119.45	0.564
	7.63				
55.45		0.20	0.835	89.86	0.544
	17.85				
73.30		0.10	0.91	48.97	0.209
	23.02				
96.32		0.05	0.945	25.43	0.05
	32.44				
128.76		0.01	0.96	5.16	0.003
	55.45				
184.21		0.005	0.97	2.60	0.001
					4.314

$$B_{OX}^{c}=538.1 N_0 f_t \ \text{kG}, \tag{16}$$

$$B_{OX}^{\text{nc}}=538.1\times(0.12\times10^{-8}) N_0 f_t \ \text{kG}. \tag{17}$$

Thus, the magnetic field increases with the product $N_0 f_t$. If we compare Eqs. (16) and (17) we see that B_{OX}^{nc} is smaller than B_{OX}^{c} by a factor 12×10^{-8} so we can neglect B_{OX}^{nc}.

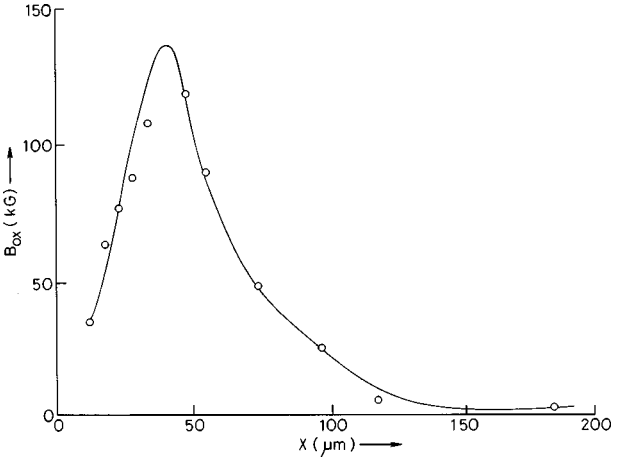

FIG. 4. Calculations of the transmission fraction (f_t) as a function of distance (x) from critical density surface.

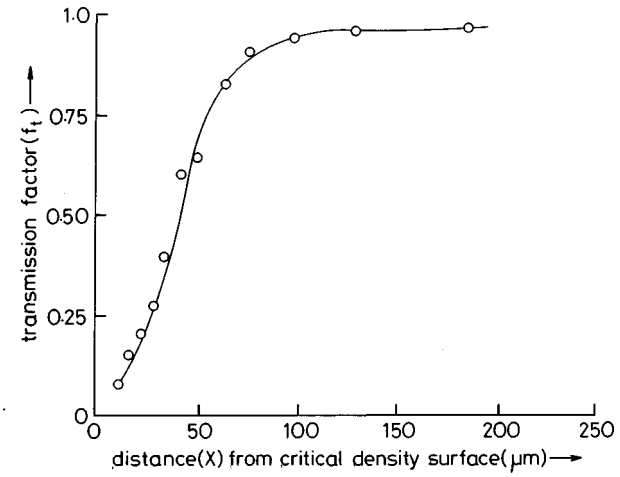

FIG. 5. Calculations of the axial field (B_{OX}) as a function of the distance (x) from the critical density surface.

The Faraday rotation angle (α), a quantity of experimental interest, is given by the formula [2]

$$\delta\alpha=0.296 N_0 B_{OX} dx, \tag{18}$$

where B_{OX} is in kG, dx is in cm, and $\delta\alpha$ is in radians,

$$\delta\alpha=1.696\times10^{-3} N_0 B_{OX} dx \ \ (\text{deg}), \tag{19}$$

$$\delta\alpha=0.9126 N_0^2 f_t dx \ \ (\text{deg}), \tag{20}$$

where dx is in the μm and B_{OX} is in kG. Thus $\delta\alpha \propto B_{OX}$.

Results are tabulated in Table I, at different positions (with respect to critical density surface), that is, at different values of N_0 and f_t.

From Table I, it is clear that the magnetic field increases monotonically as f_t increases from 0.075 to 0.6 and N_0 decreases from 0.8536 to 0.40. After that, it decreases as f_t increases from 0.6 to 0.97 and N_0 decreases from 0.40 to 0.005. So the maximum field is neither at the critical density surface nor at the end of the coronal region but in between. Consequently, Faraday rotation is higher for the slab corresponding to the maximum field. The variation of the self-generated axial magnetic field due to collisional excitation along the axial direction is shown in Fig. 4. The reasons for the maximum field at the particular position can be as follows.

If we carefully go through Eq. (16) and Figs. 3 and 5, we can visualize the facts. From Eq. (16) it is clear that the higher the $N_0 f_t$, the higher is the field. N_0 is maximum at the critical density surface and minimum at the end of the coronal region. For f_t it is just the reverse, namely, maximum in the coronal region and minimum at the critical density surface. So there is an optimum region between the two extreme points where $N_0 f_t$ is maximum. Hence the magnetic field and the Faraday rotation are higher at that region.

Taking the total coronal length as 210 μm, the net Faraday rotation is 4.314° for a single pass of the laser beam. For double pass (SBS) the rotation would thus be 8.628°. The observed Faraday rotation was 8° as seen in Fig. 2, and theoretically it is estimated as 8.628°. Hence, theoretical results are in fairly good agreement with the experimentally observed values.

VI. CONCLUSION

Collisions in laser-produced plasma generate an axial magnetic field via the ponderomotive force. These fields are prominent where the product $N_0 f_t$ is appreciable and rotate the plane of polarization of the incident laser radiation as it propagates along the axial field.

[1] M. K. Srivastava, S. V. Lawande, Manoranjan Khan, Chandra Das, and B. Chakraborty, Phys. Fluids B **4**, 4086 (1992).

[2] J. A. Stamper, K. Papadopoulos, R. N. Sudan, S. O. Dean, E. A. Mclean, and J. M. Dawson, Phys. Rev. Lett. **26**, 1012 (1971).

[3] J. A. Stamper, Laser and Part. Beams **9**, 841 (1991); C. E. Max, W. M. Manheimer, and J. J. Thomson, Phys. Fluids **21**, 128 (1978).

[4] J. A. Stamper and B. H. Ripin, Phys. Rev. Lett. **34**, 138 (1975); P. Mora and R. Pellat, Phys. Fluids **24**, 2219 (1981).

[5] B. Chakraborty, Susmita Sarkar, Chandra Das, B. Bera, and Manoranjan Khan, Phys. Rev. E **47**, 2236 (1993).

[6] L. A. Balshov, A. M. Dykhne, N. B. Kowalski, and A. I. Yudin, in *Handbook of Plasma Physics*, edited by M. Rosenbluth and R. Sagdeev (Elsevier, New York, 1991), Vol. 3, Chap. 12, pp. 518–547.

[7] J. A. Stamper and D. A. Tidman, Phys. Fluids **16**, 2004 (1973); I. Bernstein, C. E. Max, and J. J. Thomson, *ibid.* **21**, 905 (1978).

[8] Chandra Das, B. Bera, B. Chakraborty, and Manoranjan Khan, J. Plasma Phys. **50**, 191 (1994).

[9] B. Chakraborty, M. Khan, and B. Bhattacharyya, J. Appl. Phys. **59**, 1473 (1986).

[10] C. E. Max, in *Laser Plasma Interaction*, edited by R. Balian and J. C. Adams (North-Holland, Amsterdam, 1982), pp. 304–410.

[11] J. Briand, V. Adrian, M. El. Tamer, A. Gomes, Y. Quemener, J. P. Dinquirard, and J. C. Kieffer, Phys. Rev. Lett. **54**, 38 (1985).

[12] R. H. Lehmberg and J. A. Stamper, Phys. Fluids **21**, 814 (1978).

[13] R. N. Sudan, Phys. Rev. Lett. **70**, 3075 (1993).

[14] S. C. Wilks, W. L. Kruer, M. Tabak, and A. B. Langdon, Phys. Rev. Lett. **69**, 1383 (1992).

[15] Naval Research Laboratory Report No. 7838,56 (1974).

[16] R. Dragila, Phys. Rev. A **32**, 54 (1985).

[17] T. Desai, H. C. Pant, M. Khan, S. Sarkar, and B. Chakraborty, J. Plasma Phys. **51**, 211 (1994).

[18] W. L. Kruer, *Radiation in Plasmas Review from College on Plasma Physics* (unpublished), Vol. I, p. 491.

[19] M. Khan, S. Sarkar, B. Bhattacharya, B. Chakraborty, T. Desai, and H. C. Pant, J. Appl. Phys. **72**, 2199 (1992).